Towards a Pixel TPC part II: performance of a 32 chip GridPix detector

M. van Beuzekom[a], Y. Bilevych[b], K. Desch[b], S. van Doesburg[a], H. van der Graaf[a], F. Hartjes[a], J. Kaminski[b], P.M. Kluit[a], N. van der Kolk[a], C. Ligtenberg[a], G. Raven[a], J. Timmermans[a]

[a]*Nikhef, Science Park 105, 1098 XG Amsterdam, The Netherlands*
[b]*Physikalisches Institut, University of Bonn, Nussallee 12, 53115 Bonn, Germany*

Abstract

A Time Projection Chamber (TPC) module with 32 GridPix chips was constructed and the performance was measured using data taken in a testbeam at DESY in 2021. Part I of the results were described in a previous paper. The analysed data were taken at electron beam momenta of 5 and 6 GeV/c and at magnetic fields of 0 and 1 Tesla(T).

Keywords: Micromegas, gaseous pixel detector, micro-pattern gaseous detector, Timepix, GridPix, pixel time projection chamber

1. Introduction

As a step towards a Pixel Time Projection Chamber for a future collider experiment [5], [6], a module consisting of 32 GridPix chips based on the Timepix3 chip was constructed. The GridPix chips have a very fine granularity of 55x55 μm^2 and a high efficiency to detect single ionisation electrons.

The 32 GrixPix chip module was put in a test beam at DESY and complemented with two sets of Mimosa26 silicon detector planes. The analysed data were taken at electron beam momenta of 5 and 6 GeV/c and at magnetic fields of 0 and 1 T.

A description of the constrution of the GridPix module, the test beam setup and data taking conditions can be found in part I of our paper [3]. The paper

*Corresponding author. Telephone: +31 20 592 2000
Email address: s01@nikhef.nl (P.M. Kluit)

explains the track reconstruction procedure and the precise TPC tracking results that were obtained.

2. Analysis topics

In the following sections the analysis results for different topics will be presented. Firstly, the particle identification performance using dE/dx or dN/dx will be measured. Secondly, the single electron efficiency at high hit rates will be determined. Thirdly, the characterisation of large hit bursts caused by highly ionizing particles will be presented. Fourth, the resolution in the precision plane as a function of the incident track angle will be measured. Finally, the projected dE/dx performance for a Pixel TPC in the ILD experiment will be presented and discussed.

2.1. Particle Identification using dE/dx or dN/dx

The distribution of the number of TPC track hits per chip for the B = 0 T and for the B = 1 T data sets are a starting point for a measurement of the dE/dx or dN/dx performance. As was shown in Part I of the paper [3], the mean number of hits is measured to be 124 and 89 in the B = 0 T and 1 T data sets respectivelly. The most probable values are respectively 87 and 64.

In order to measure the track performance of dE/dx or dN/dx, the central chips - defined in ref [3] - were selected and calibrated to give the same mean number of hits per chip. By combining the hits associated to the track, a new 1 m long track is formed. The 1 m long track has a coverage of 60% because inactive regions (chip edges and e.g. guard) are included. By applying different analysis methods, the dE/dx or dN/dx resolution can be measured from data.

The first method rejects large clusters with more than 6 hits in 5 consecutive pixels. Finally a dE/dx truncation at 90% is performed using samples of 20 pixels; so the 10% largest dE/dx values are removed and dE/dx re-estimated. This method doesnot fully exploit the full granularity of the pixel TPC.

The second method exploits the distribution of the minimum distance in the pixel plane between consecutive hits. If only single electron clusters were made in a gas, one would expect an exponentially falling distance distribution. Multi-electron clusters will give rise to a peak at low distances tthat is smeared out by the transverse diffusion process. The slope of the exponential distribiution is proportional to the dN/dx i.e. the clusters produced by the electron. The long Landau tail in the dE/dx distribution is coming from the multi-electron clusters that peak at low distances.

Using a large number of tracks, it is possible to measure from data the shape of the minimum distance distribution. At distances above 10 pixels the distribution follows an exponential distribution. At lower distance weights for the B = 0 T and 1 T data are determined and applied to ensure an exponential distribution over the whole range. Finally, per 1 m track, a fit to distance distribution in data is performed with the following template function:

$$N(d_{xy}) = N_0 \text{ weight}(d_{xy})\ e^{-\text{slope } d_{xy}}. \tag{1}$$

where d_{xy} is the minimum distance in the precision plane (xy). The slope and N_0 - normalisation - are left free in the per track fit, the weights are fixed using the whole data set.

The testbeam data provides a dE/dx or dN/dx measurement for electrons. The data were also used to perform a measurement of response of a MIP particle - here defined as a particle that produced 70% of the electron dE/dx. By dropping 30% of the hits associated to the track and applying the two methods, the performance could be measured and the linearity of the technique tested.

The relative resolution is defined as the r.m.s. of the distribution divided by the mean and the results are shown in Table 1. The resolution of the B= 1 T data is about 40% better than the B= 0 data. This is consistent with the smaller fluctuations that are present in the distributions of the number of hits per chip in the B= 1T data [3]. The template fit method has in the B= 1T data a 20% better performance than the dE/dx truncation method. One might argue that with more diffusion the results from the template fit method will move more towards the results of the dE/dx truncation method. Note however that the diffusion contribution to the track resolution in the 1 T data is already

Table 1: dE/dx or dN/dx resolution for different methods and data sets

Method	B=0 T resolution	B=1 T resolution
-	%	%
1 dE/dx truncation	6.0	3.6
2 template fit	5.4	2.9

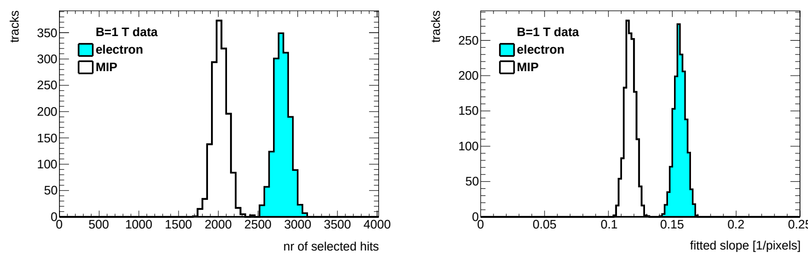

Figure 1: Distribution of the number of selected hits (left) for the dE/dx truncation method and the fitted slope (right) for the template fit method for an electron (light blue shaded) and MIP 1 m lomg tracks with 60% coverage for the B = 1 T data.

sizeable compared to the pixel size and varies between 85-150 μm.

The results for the 1 T data are shown in Figure 1 for electrons and MIPs for $dE/dxtruncation$ and $templatefit$ methods. The linearity - defined as the mean MIP response divided by the mean electron response divided by 0.7 - was measured to be 1.03 for method 1 and 1.07 for method 2. This value is slightly different from 1, and can be corrected for by scaling the expected values for different particles as a function of the measured momentum.

The performance result of the 32 chip GridPix detector is impressive. It has currently, the best performance (running at atmospheric pressure) of constructed TPCs - and demonstrates the particle identification capabilities of a GridPix Pixel TPC.

2.2. Single electron efficiency at high hit rates

The efficiency of the device to detect a hit in a high (low) rate environment is measured comparing the mean time over threshold for low and high rate

Table 2: Mean time of threshold and rates for different runs

run	B	ToT 1	ToT 2	triggers	run time	Hits 1	Hits 2	trig rate	Rate 1	Rate 2
	T	μs	μs	10^3	10^3s	10^6	10^6	Hz	hits/s	hits/s
6916	0	0.628	0.653	16.8	23.2	6.25	13.1	0.72	269	565
6934	0	-	0.651	73.4	2.41	-	20.5	30.4	-	8479
6935	0	0.620	-	7.39	2.41	6.95	-	30.6	2878	-
6969	1	0.650	0.666	7.94	13.8	1.93	2.16	0.57	139	156
6983	1	0.657	0.678	6.79	2.83	11.6	14.1	24.1	4110	4986

runs at B fields of 0 and 1 T. The mean time over threshold is sensitive to the single electron efficiency of the detector. In order to extract a precise result, hits associated to TPX3 tracks were used. The track selection is the same as the one that was described in the subsection on the particle identification performance. The analysed runs for the B=0 T data set were runs 6916, 6934 and 6935 and for the B=1 T data set run 6969 and 6983.

For each run the mean ToT values were measured for values between 0.15 and 1.4 μs. These cuts were applied to remove the noise and the tail.

The results for the measured average time over threshold for different runs and hit rates are summarised in Table 2. ToT 1(2) denotes the mean time over threshold for upper and lower half of the module and Hits 1(2) corresponds to number of recorded raw hits. The mean Rate 1 (2) was calculated dividing the total number of raw hits by the total run time. For the B=0 T data two high rate runs 6934 and 6935 had to be analysed because the beam crossed either the upper or the lower part of the module and therefore no measurement could be performed (denoted by -). The statistical uncertainties are - due to the high statistics - negligible.

The relative change in the mean time over threshold for the B=0 data is -1.2% (upper) and -0.3% (lower). In this case the rate goes up to 8.5 kHz for 6 chips or 1.4 kHz per chip. The relative change in the mean time over threshold for the B=1 T data is +1% (upper) and +1.7% (lower) The rate goes up to 5 kHz for 6 chips or 1.2 kHz per chip.

The relative change in the mean time over thresholds δToT/ToT can be related to the relative change in the single electron efficiency $\delta\epsilon/\epsilon$ by:

$$\delta\text{ToT}/\text{ToT} = \text{c}\ \delta\epsilon/\epsilon. \tag{2}$$

The slope c is about 0.5 at the mean working point of ToT=0.65 μs and is determined from the measured efficiency-ToT curve in [5].

This means that the relative efficiency is stable at the level of +0.9% (B=1 T) and -0.6% (B=0T) for hit rates up to 1.2 (1.4) kHz per chip. To connclude, running at hit rates up 1.4 kHz per chip gives at most a reduction of 0.6% in the relative efficiency.

2.3. Characterisation of hit bursts

In event displays large hit burst caused by highly ionizing particles (e.g. alpha's or delta electrons) can be observed. A Pixel TPC is well suited to study and characterize these typical hit bursts. A pixel TPC also allows to improve the high momentum tracking by removing these bursts.

To study the hits burst the data of run 6969 B=1 T was analysed. No acceptance or track selection cuts were applied. A burst was selected with more than 100 hits in a radius of 50 pixels around the burst center within a time window of 200 ns around the mean time. The mean position in xy and the mean time of the burst were iteratively estimated. The bursts were characterized by the number of associated hits, the radius in which 90% of the hits are found (radius90) and the time in which 90% of the hits are detected (time90).

The distributions for radius90 and time90 for different burst sizes are shown in Figure **??**.

For high momentum tracking it is important to cut tightly on the track residuals in xy and z. In particular the cut in z reduces the impact of bursts in the B=1 T data. One could in addition run a burst finding algorithm and downweight the hits associated to burst and the selected track. This will remove biases and improve the track parameter estimation.

2.4. Resolution study

Here, the resolution in the precision plane as a function of the incident track angle will be measured.

2.5. Projected dE/dx performance

Here, the projected dE/dx performance for a Pixel TPC in ILD will be presented.

3. Conclusion and outlook

Acknowledgements

This research was funded by the Netherlands Organisation for Scientific Research NWO. The authors want to thank the support of the mechanical and electronics departments at Nikhef and the detector laboratory in Bonn. The measurements leading to these results have been performed at the Test Beam Facility at DESY Hamburg (Germany), a member of the Helmholtz Association (HGF).

References

[1] C. Ligtenberg, et al., Performance of a GridPix detector based on the Timepix3 chip, Nucl. Instrum. Meth. A 908 (2018) 18–23. arXiv:1808.04565, doi:10.1016/j.nima.2018.08.012.

[2] C. Ligtenberg, et al., Performance of the GridPix detector quad, Nucl. Instrum. Meth. A 956 (2020) 163331. arXiv:2001.01540, doi:10.1016/j.nima.2019.163331.

[3] M. van Beuzekom, et al., Towards a Pixel TPC part I: construction and test of a 32 chip GridPix detector, submitted to Nucl. Instrum. Meth. A.

[4] J. Kaminski, Y. Bilevych, K. Desch, C. Krieger, M. Lupberger, GridPix detectors - introduction and applications, Nucl. Instrum. Meth. A845 (2017) 233–235. doi:10.1016/j.nima.2016.05.134.

[5] C. Ligtenberg, A GridPix TPC readout for the ILD experiment at the future International Linear Collider, Ph.D. thesis, Free University of Amsterdam (2021).
URL https://www.nikhef.nl/pub/services/biblio/theses_pdf/thesis_C_Ligtenberg.pdf

[6] M. Lupberger, Y. Bilevych, H. Blank, D. Danilov, K. Desch, A. Hamann, J. Kaminski, W. Ockenfels, J. Tomtschak, S. Zigann-Wack, Toward the Pixel-TPC: Construction and Operation of a Large Area GridPix Detector, IEEE Trans. Nucl. Sci. 64 (5) (2017) 1159–1167. doi:10.1109/TNS.2017.2689244.

[7] T. Poikela, J. Plosila, T. Westerlund, M. Campbell, M. De Gaspari, X. Llopart, V. Gromov, R. Kluit, M. van Beuzekom, F. Zappon, V. Zivkovic, C. Brezina, K. Desch, Y. Fu, A. Kruth, Timepix3: a 65K channel hybrid pixel readout chip with simultaneous ToA/ToT and sparse readout, JINST 9 (05) (2014) C05013.
URL http://stacks.iop.org/1748-0221/9/i=05/a=C05013

[8] J. Visser, M. van Beuzekom, H. Boterenbrood, B. van der Heijden, J. I. Muñoz, S. Kulis, B. Munneke, F. Schreuder, SPIDR: a read-out system for Medipix3 & Timepix3, Journal of Instrumentation 10 (12) (2015) C12028. doi:10.1088/1748-0221/10/12/C12028.

[9] B. van der Heijden, J. Visser, M. van Beuzekom, H. Boterenbrood, S. Kulis, B. Munneke, F. Schreuder, SPIDR, a general-purpose readout system for pixel ASICs, JINST 12 (02) (2017) C02040. doi:10.1088/1748-0221/12/02/C02040.

[10] F. Hartjes, A diffraction limited nitrogen laser for detector calibration in high energy physics, Ph.D. thesis, University of Amsterdam (1990).
URL https://www.nikhef.nl/pub/services/biblio/theses_pdf/thesis_F_Hartjes.pdf

[11] R. Diener et al., The DESY II test beam facility, Nuclear Instruments and Methods in Physics Research. Section A: Accelerators, Spectrometers, Detectors and Associated Equipment 922 (2019) 265–286. arXiv:1807.09328, doi:10.1016/j.nima.2018.11.133.

[12] P. Baesso, D. Cussans, J. Goldstein, The AIDA-2020 TLU: a flexible trigger logic unit for test beam facilities, Journal of Instrumentation 14 (09) (2019) P09019–P09019. arXiv:2005.00310.
URL https://doi.org/10.1088/1748-0221/14/09/p09019

[13] D. Dannheim, K. Dort, L. Huth, D. Hynds, I. Kremastiotis, J. Kröger, M. Munker, F. Pitters, P. Schütze, S. Spannagel, T. Vanat, M. Williams, Corryvreckan: a modular 4d track reconstruction and analysis software for test beam data, Journal of Instrumentation 16 (03) (2021) P03008. doi:10.1088/1748-0221/16/03/p03008. arXiv:2011.12730.
URL https://doi.org/10.1088/1748-0221/16/03/p03008

[14] R. Veenhof, Garfield - simulation of gaseous detectors, version 9, Reference W5050 (1984-2010).
URL https://garfield.web.cern.ch

[15] C. Kleinwort, General broken lines as advanced track fitting method, Nuclear Instruments and Methods in Physics Research Section A: Accelerators, Spectrometers, Detectors and Associated Equipment 673 (2012) 107–110. doi:10.1016/j.nima.2012.01.024.

[16] S. F. Biagi, Monte Carlo simulation of electron drift and diffusion in counting gases under the influence of electric and magnetic fields, Nucl. Instrum. Meth. A421 (1-2) (1999) 234–240. doi:10.1016/S0168-9002(98)01233-9.
URL https://magboltz.web.cern.ch/magboltz